Development of a design methodology to maximize exergy density of compressed air storage vessels

Markus Hadam[a], Marcus Budt[b], Sven Klute[c], Matthias Lehmkühler[d]

[a] *Fraunhofer Institute UMSICHT, Oberhausen, Germany, markus.hadam@umsicht.fraunhofer.de*
[b] *Fraunhofer Institute UMSICHT, Oberhausen, Germany, marcus.budt@umsicht.fraunhofer.de*
[c] *Fraunhofer Institute UMSICHT, Oberhausen, Germany, sven.klute@umsicht.fraunhofer.de*
[d] *Fraunhofer Institute UMSICHT, Oberhausen, Germany, matthias.lehmkuehler@umsicht.fraunhofer.de*

Abstract:

The increasing share of intermittent renewable energy sources drives the demand for flexible energy storage technologies, among which compressed air energy storage (CAES) represents a promising option for medium- to large-scale applications. A critical cost driver of above-ground CAES systems is the isochoric compressed air storage (CAS) vessel, whose economic viability depends on maximizing the volumetric exergy density – defined as the maximum recoverable work per unit storage volume – through optimal pressure design.

This study presents a generalized, layout-independent thermodynamic methodology to determine the maximum achievable exergy density of isochoric CAS as a function of maximum storage pressure (up to 400 bar), operable pressure bandwidth (up to 240 bar), and storage temperature (up to 100 °C), using real-gas property data for dry air. The analysis reveals that, for any given combination of pressure bandwidth and storage temperature, a thermodynamically optimal maximum storage pressure exists that maximizes exergy density. For a pressure bandwidth of 20 bar at 15 °C, this optimum is located at approximately 150 bar, leading to an exergy density of 2.52 kWh/m³. This effect is related to the reduced compressibility of air elevated pressures and thus cannot be captured by the ideal gas assumption, which overestimates the exergy density above approximately 120 bar.

The results illustrate that the operable pressure bandwidth is the key design parameter for exergy density and has a significantly greater influence than the maximum storage pressure. Furthermore, elevated storage temperatures reduce the achievable exergy density by up to 23 % and shift the optimum maximum pressure toward higher pressures. Based on these findings, a performance map of exergy density isolines is developed, providing a practical planning tool for the early-stage thermodynamic design of isochoric CAS. The map enables rapid identification of favourable pressure operating windows, independent of specific CAES plant configurations. Moreover, since the methodology is based on general thermodynamic principles, it is transferable to other technically relevant gas storages like for carbon dioxide.

Keywords:

Compressed air energy storage, Exergy, Exergy density, Isochoric storage

1. Introduction

1.1. Current state of R&D

The first two commercial compressed air energy storage (CAES) plants were commissioned in Huntorf, Germany (1978) and McIntosh, USA (1991) [1, 2]. Both represent diabatic CAES (D-CAES), in which compression heat is dissipated to the environment and the combustion of natural gas is used to reheat the compressed air prior to expansion.

Despite this early commercialization, no further plants were built for several decades. Nevertheless, sustained research and development efforts demonstrate that CAES remains a relevant technology for medium- to long-duration energy storage. In recent years, a number of demonstration plants have been commissioned worldwide [3–7]. Furthermore, some commercial plants were built recently, especially in China [7–10]. In addition, many studies have been published in recent decades. As summarized in [5, 7, 11–13], these studies investigate different plant layouts regarding thermodynamics by means of analytical methods and simulation. The main goals are to analyse the complex thermodynamic processes of CAES systems and to identify potential for improvement.

Beyond D-CAES, three thermodynamically different CAES variants have been extensively investigated. In adiabatic CAES (A-CAES), compression heat is captured in a thermal energy storage (TES) and used to heat up the pressurized air prior to expansion, thereby enabling higher round-trip efficiencies. Isothermal CAES (I-CAES) pursues near-constant temperature operation throughout compression and expansion via enhanced heat transfer, approaching the thermodynamic optimum of reversible isothermal processes and theoretically surpassing the efficiency of adiabatic approaches [11]. In liquid air energy storage (LAES), air is liquefied cryogenically and stored at near-atmospheric pressure in insulated cryogenic vessels. This increases the volumetric exergy density but also reduces the efficiency compared to A-CAES systems. Since LAES operates on fundamentally different thermodynamic and storage principles, it is excluded from the scope of this study, which focuses exclusively on CAES systems.

1.2. Compressed air storage vessels

A critical challenge for D-CAES, A-CAES, and I-CAES is the high specific investment cost associated with the compressed air storage (CAS) vessel. Large-scale approaches of all three concepts typically rely on underground geological formations – primarily salt caverns or aquifers – to provide high-volume air storage. While the initial CAPEX for developing such formations is significant, the surrounding rock mass serves as natural pressure containment, resulting in low specific costs for large storage capacities. However, the geographical dependence on suitable formations, combined with the high volume-specific investment cost per unit of stored exergy at lower capacities, limits their applicability, particularly for smaller, decentralized plants. For small-scale CAES (< 15 MW), constructed CAS technologies with smaller storage vessels such as underwater (isobaric) or aboveground (typically isochoric) CAS systems are viable alternatives [7, 14–19]. Since the latter can be installed independently of geographical constraints, this study focuses on aboveground isochoric CAS.

Aboveground storage systems rely on constructed pressure vessels, such as steel cylinders, spheres or pipes, whose specific cost is significantly higher than that of large-scale underground formations [14, 16, 18, 20] Consequently, volumetric exergy density serves as a key performance indicator for isochoric CAS and directly determines the economic competitiveness of above-ground CAS. Furthermore, abandoned mines and existing pipe networks represent potential alternatives for small-scale compressed air storage, thereby reducing the investment costs.

1.3. Exergetic density of CAS

The exergy density of an isochoric CAS depends on the maximum pressure, the operable pressure bandwidth, and the storage temperature, as well as on the thermal behaviour during the charging, storing, and discharging processes. Salt caverns have a relatively low exergy density, as the maximum pressure and the operable pressure bandwidth (usually Δp_{max} = 20 bar) are geologically limited. For example, operation between 46 and 66 bar (as in the Huntorf plant) results in an exergy density of 2.25 kWh/m³ [21]. By contrast, constructed storage systems such as steel pipe storage can be designed with significantly greater flexibility and thus achieve higher exergy densities.

Only a few studies focus on the energy and exergy density of compressed air storage systems. Cárdenas et al. [18] introduce the use of a wire-wound pressure vessel for small-scale CAES and investigate the exergy density of compressed air as a function of the maximum storage pressure, focusing on isobaric operation. Isochoric operation between 100 and 250 bar under ideal (isothermal) conditions yields an exergy density of 21.3 kWh/m³, whereas an isobaric configuration achieves 56.2 kWh/m³ at a pressure of 250 bar. White [21] analyses the trade-off between cycle efficiency and exergy density for isobaric and isochoric caverns, using a throttle valve to maintain an operation of the turbomachinery at the design point. An exergy density of 5.44 kWh/m³ at a pressure operation of 50–100 bar is calculated considering a volumetric efficiency of 0.9.

He et al. [15] investigate the stored exergy for a Huntorf CAES layout with a pressure range of 43 to 70 bar for different heat transfer conditions of the cavern including isotherm, convective heat transfer and adiabatic wall conditions. Isothermal behaviour leads to an exergy density of 2.79 kWh/m³, convective heat transfer to 2.37 kWh/m³, and adiabatic conditions to 2.01 kWh/m³. Accordingly, realistic considering realistic convective heat transfer and adiabatic conditions reduce the exergy density by 15.1 % and 28.0 %, respectively, compared to isothermal conditions.

Guo et al. [22] analyse the exergy density for a specific A-CAES using five compression stages and a throttle valve to maintain a constant air pressure in the expansion line. The exergy density is analysed as a function of the maximum storage pressure (80–200 bar) and the pressure after the throttle valve (0–140 bar), yielding values between 5.0 and 17.2 kWh/m³ based on real gas property data of air. Furthermore, it is shown that temperature fluctuations in the CAS should be considered, as they can reduce the exergy density by 8.7–27.2 %.

The aforementioned studies provide a valuable overview of achievable exergy densities for CAES systems. However, these analyses are constrained by specific technical design assumptions – such as the use of throttle valves, fixed turbomachinery operating points, or defined number of compression and expansion stages – which limits their general applicability and comparability across different CAS configurations. To enable a generalized and system-independent evaluation, this work presents a fundamental thermodynamic analysis of the volumetric exergy density of an isochoric CAS volume, decoupled from any specific CAES layout to determine the optimal pressure design.

2. Thermodynamic assumptions and fundamentals

This chapter introduces the thermodynamic framework used to analyse the exergy density of an isochoric CAS as a function of maximum pressure, pressure bandwidth, and storage temperature. The following assumptions are made:

1. Isothermal storage process: The compressed air storage is charged under ideal (isothermal) conditions, resulting in maximum volumetric efficiency.
2. Real gas behaviour of dry air: Real gas property data of dry air are considered using the property library LibHuAir [23], since the behaviour of air at high pressures deviates significantly from the ideal gas assumption.
3. Isochoric operation: The CAS operates at constant volume. Therefore, the stored exergy is determined by the maximum pressure, pressure bandwidth and storage temperature.
4. Aboveground storage: The focus is on constructed pressure vessels rather than geological formations such as salt caverns. Consequently, no geological constraints on the maximum pressure or bandwidth apply.
5. Ambient conditions: The ambient conditions are set to t_a = 15 °C and p_a = 1.01325 bar

Real gas behaviour and compressibility factor

The thermodynamic behaviour of air at elevated pressures deviates from the ideal gas law ($pV_m = nRT$) due to intermolecular interactions. This deviation is quantified by the compressibility factor Z, defined as the ratio of the actual molar volume V_m to the ideal gas molar volume (RT/p) at the same temperature T and pressure p according to Eq. (3.1).

$$Z = \frac{pV_m}{RT} \qquad (3.1)$$

For an ideal gas, the compressibility factor is Z = 1. For real gases, the compressibility factor is a function of pressure and temperature. At moderate pressures, the compressibility factor of air is Z < 1, meaning the gas is more compressible than predicted by the ideal gas law leading to a higher density for a given pressure. At elevated pressures (60–80 bar for air at 15 °C), repulsive interactions between molecules dominate, leading to a compressibility factor of Z > 1. In this regime, the gas becomes progressively less compressible resulting in a reduced density for a given pressure.

Specific exergy and density relationships

The usable exergy of compressed air stored in a CAS depends fundamentally on two properties: the specific exergy of the gas and the density variation achievable within the operational pressure range. In the exergy analysis of CAES, the chemical, kinetic, and potential exergy components of the specific exergy of a material flow are negligible. Thus only the term of physical exergy e remains for the determination of the exergy of the material flow according to Eq. (3.2). [11, 24]

$$e = h - h_a - T_a(s - s_a) \qquad (3.2)$$

Therefore, the specific physical exergy e is a function of the thermodynamic state variables (enthalpy h, entropy s) of the considered material flow and is strictly related to the reference ambient conditions (h_a, s_a, T_a). The exergy density e_d describes the maximum usable work per unit volume of a stored gas and is a key parameter for evaluating gas storage systems. It is calculated from the stored exergy E and the storage volume V according to Eq. (3.3).

$$e_d = \frac{E}{V} \qquad (3.3)$$

For isochoric storage systems, the exergy density e_d is calculated by integrating the specific exergy e_{ph} with respect to density over the operational density range $d\rho$, which is determined by the maximum storage pressure p_{max} and the pressure bandwidth Δp (Eq. 3.4).

$$e_d = \int_{\rho_{p,max-\Delta p}}^{\rho_{p,max}} e(p,t)\, d\rho \qquad (3.4)$$

3. Results

This chapter presents the behaviour of the specific exergy, density, and the resulting exergy density of an isochoric CAS as a function of maximum pressure, pressure bandwidth, and storage temperature.

3.1. Specific exergy and stored mass in isochoric CAS

The exergy density e_d of an isochoric gas storage is a function of the pressure and temperature dependent specific exergy and density. For illustrative purposes, the following analysis assumes a CAS with a pressure bandwidth of Δp = 20 bar, corresponding to a typical value for salt caverns operations.

For real gas behaviour under isothermal conditions, the specific exergy e increases with pressure following a characteristic nonlinear trend (Figure 1): At lower pressures, specific exergy exhibits rapid initial growth, which gradually reduces at higher pressures. This behaviour reflects the diminishing marginal gain in mechanical exergy at high pressures, analogous to the logarithmic pressure dependence known from ideal gas thermodynamics. Higher storage temperatures in a realistic range increase the specific exergy only marginally. Across the pressure range up to 400 bar, the specific exergy at a storage temperature of 100 °C is 3.2 % higher than at ambient conditions. At higher pressures, the relative impact decreases due to the increased pressure related exergy contribution.

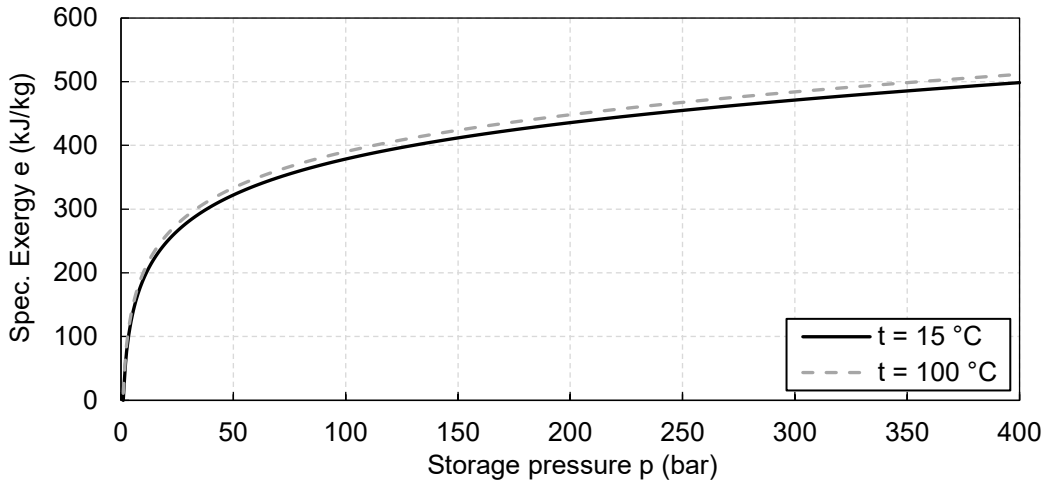

Figure 1: Specific exergy of dry air as a function of pressure for storage temperatures of 15 °C and 100 °C.

If the specific exergy is plotted as a function of density, the volumetric exergy density e_d can be represented graphically according to Eq. 3.4 (Figure 2). For a temperature of t = 15 °C, storage pressure of p_{max}= 100 bar and a pressure bandwidth of Δp = 20 bar, the exergy density is 2.52 kWh/m³. Increasing the maximum pressure while maintaining a constant pressure bandwidth shifts the enclosed area toward higher pressures, thereby increasing the specific exergy. However, to determine whether this results in a net increase in exergy density, the pressure dependence of density must be examined.

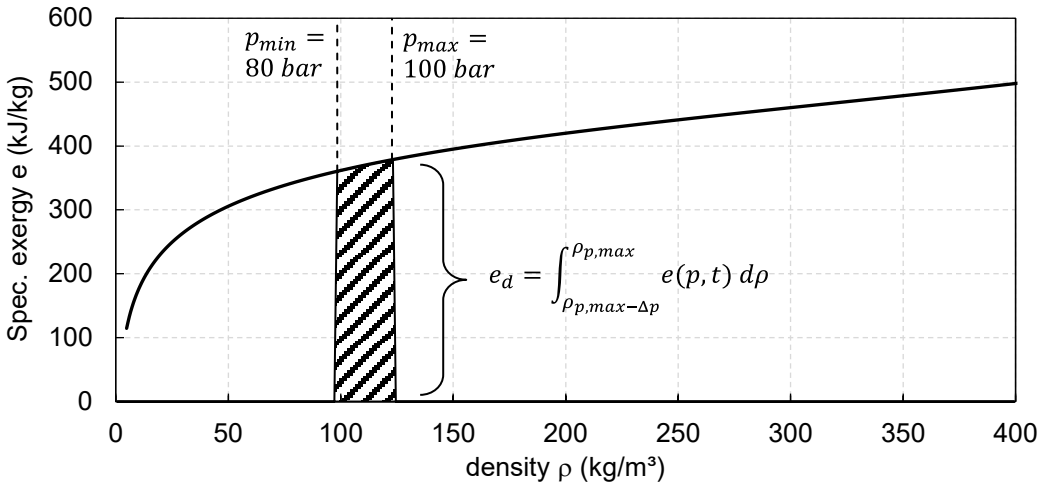

Figure 2: Specific exergy of dry air as a function of density for storage temperatures of 15 °C; Integral for an operating pressure range of p_{min} = 80 bar (ρ_{min} = 98.4 kg/m³) and p_{max} = 100 bar (ρ_{max} = 122.8 kg/m³).

As shown in Figure 3, the density of air increases steadily with rising pressure; however, the slope decreases slightly at higher pressures due to the rising compressibility factor of air (Z > 1). This effect is further illustrated by the change in density ($\Delta\rho_1$ = 24.47 kg/m³, $\Delta\rho_2$ = 14.71 kg/m³) shown in Figure 3 for different maximum pressures (p_1 = 100 bar, p_2 = 350 bar) with equal pressure bandwidths of $\Delta p_1 = \Delta p_2$ = 20 bar. Under ideal gas conditions, the compressibility factor is equal to one, which results in a linear relationship between density and pressure (see grey dashed line in Figure 3). For this reason, the change in density for the given pressure bandwidth of Δp = 20 bar remains constant at 24.18 kg/m³ across the entire pressure range.

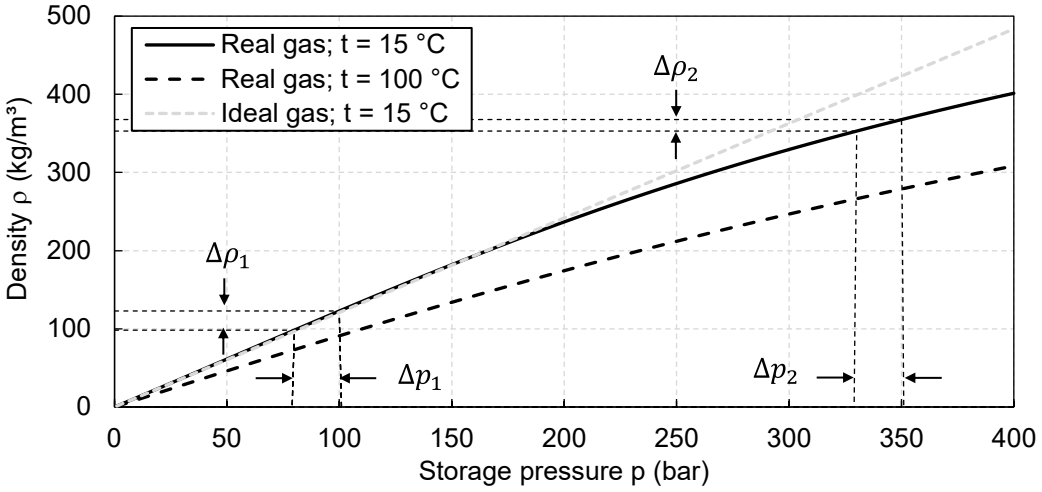

Figure 3: Density of dry air as a function of pressure for storage temperatures of 15 C and 50 °C; p_1 = 100 bar, p_2 = 350 bar, $\Delta p_1 = \Delta p_2$ = 20 bar, $\Delta\rho_1$ = 24.47 kg/m³; $\Delta\rho_2$ = 14.71 kg/m³.

Figure 4 illustrates the two fundamental terms governing the volumetric exergy density as functions of maximum storage pressure p_{max} for a fixed pressure bandwidth Δp at isothermal conditions. The specific exergy e increases continuously while the change in density $\Delta\rho = \rho(p_{max}) - \rho(p_{min})$ initially increases with pressure, reaches a maximum at approximately 64 bar (for air at 15 °C), and subsequently decreases since the compressibility of air declines at higher pressures. The initial rise in the change in density at low pressures is explained by the intermolecular attractive forces in air, which slightly enhance compressibility (Z < 1), whereas at elevated pressures repulsive interactions dominate (Z > 1), progressively reducing the density gain per unit pressure increment (see Eq. 3.1).

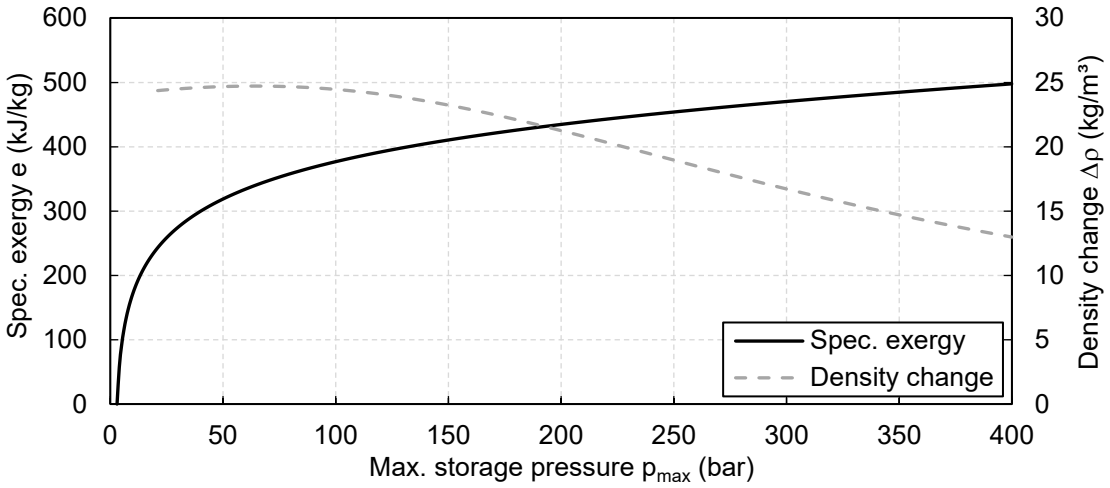

Figure 4: Specific exergy and change in density of dry air as a function of maximum storage pressure for a pressure bandwidth of Δp = 20 bar and a storage temperature of t = 15 °C.

3.2. Exergy density of isochoric CAS

The volumetric exergy density e_d is governed by the specific exergy e and density change $\Delta\rho$. These opposing trends – rising specific exergy versus declining density change at high pressures (Figure 4) – lead to the existence of an optimal maximum storage pressure that maximizes exergy density for any given pressure bandwidth and storage temperature (Figure 5). For a storage temperature of 15 °C and a pressure bandwidth of Δp =20 bar, the maximum exergetic density is e_d = 2.52 kWh/m³ at a maximum storage pressure of approximately 150 bar.

The effect of storage temperature on the exergy density is also shown in Figure 5. A higher storage temperature of 100 °C reduces the maximum exergy density by 21.8 % and shifts the optimal storage pressure to 168 bar. This is primarily caused by the reduced density slope (see Figure 3) and the consequently smaller change in density at elevated temperatures, which outweigh the marginal increase in specific exergy.

When air is treated as an ideal gas, the exergy density does not exhibit an optimum but increases continuously with rising maximum pressure, since the compressibility factor of air remains constant at Z = 1. This leads to an overestimation of the exergy density at storage pressures above approximately 120 bar.

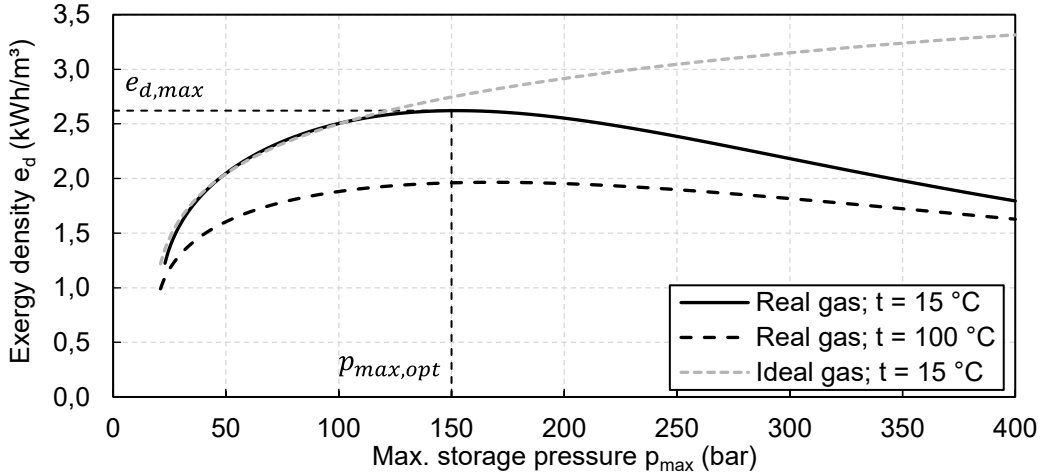

Figure 5: Exergy density as a function of maximum storage pressure for a pressure range of Δp = 20 bar and a storage temperature of t = 15 °C and t = 100 °C with a maximum exergy density of e_d= 2.52 kWh/m³ at a maximum storage pressure of p_{max} = 150 bar.

Figure 6 illustrates the dependence of the exergy density e_d on the maximum storage pressure p_{max} for various pressure bandwidths Δp at a storage temperature of 15 °C. For each curve, a distinct optimum in p_{max} is observed, and the optimal maximum storage pressure increases with the pressure bandwidth. Furthermore, increasing the pressure bandwidth results in a significantly greater increase in exergy density than raising the maximum storage pressure. The reason is that a wider pressure bandwidth directly increases the mass of air that can be charged and discharged into and out of a fixed volume, thereby raising the stored exergy.

Increasing the storage temperature to 50 °C and 100 °C reduces the exergy density within the pressure range under consideration by 11.0 % and 23.5 %, respectively.

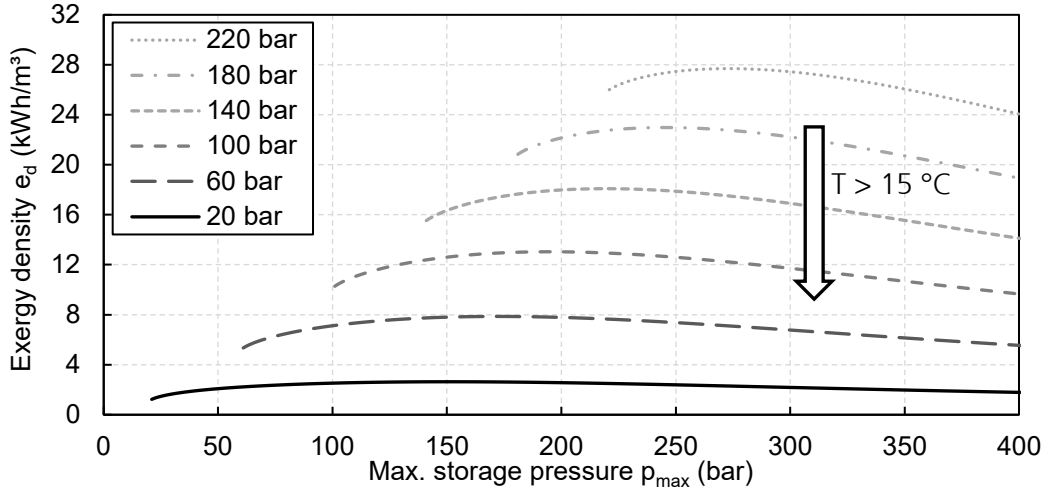

Figure 6: Exergy density as a function of maximum storage pressure for various pressure bandwidths and a storage temperature of t = 15 °C

Once the key operating conditions for a gas storage are known (target pressure bandwidth and storage temperature), the optimal maximum storage pressure required to achieve the maximum specific exergy density can be determined (Figure 7). Depending on the operating limits of the selected compressors and expanders, as well as the technical constraints of the storage system, the thermodynamically optimal maximum storage pressure may not always be achievable in practice. Consequently, it is useful to analyse isolines of exergy density, which are shown in Figure 7 over the range from ρ_d = 2.5–27.5 kWh/m³ as a function of maximum storage pressure p_{max} and pressure bandwidth Δp. The isolines provide a helpful basis for identifying and evaluating suitable design options for CAS to achieve high exergy densities and thereby reduce the overall CAPEX of CAES systems.

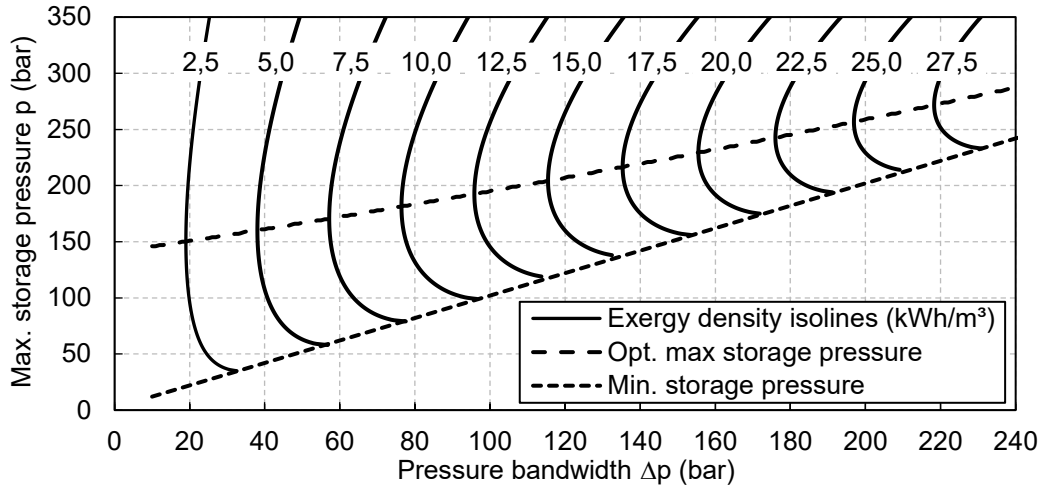

Figure 7: Performance map of exergy density isolines with optimal maximum storage pressure as a function of the pressure bandwidth for a storage temperature of t = 15 °C.

4. Discussion

The results reveal three principal findings regarding the exergy density of isochoric compressed air storage: (i) a thermodynamically optimal maximum storage pressure exists for each combination of pressure bandwidth and storage temperature, (ii) the pressure bandwidth exerts a considerably stronger influence on exergy density than the maximum storage pressure, and (iii) the ideal gas assumption fails to capture these effects at pressures above approximately 120 bar. In the following, these findings are placed in the context of existing literature, and the practical implications as well as the limitations of the method are discussed.

Comparison with existing literature and novelty of the approach

The observation that the pressure bandwidth governs the exergy density more strongly than the maximum storage pressure is consistent with the trends reported in [15, 18, 21, 22]. However, these prior analyses were conducted for specific CAES layouts – including fixed numbers of compression and expansion stages, throttle valves, and particular heat management strategies – and therefore do not investigate the thermodynamic behaviour of the CAS itself. By evaluating the CAS independently of any specific plant design and under ideal isothermal conditions over a wide parameter space (p_{max} up to 400 bar, Δp up to 240 bar), this study provides a systematic, layout-independent analysis and thereby determines the theoretical upper bound of achievable exergy density for different pressure designs.

The existence of an optimal maximum storage pressure has not been reported in prior work. Most existing studies either operate in a pressure range where the compressibility effect is not yet pronounced or employ the ideal gas assumption, which does not account for the increasing compressibility factor ($Z > 1$) that causes the density gain to dimmish at elevated pressures. The practical implication is that designing storage vessels with pressures significantly above the identified optimum increases wall thickness and thus cost without yielding a thermodynamic benefit. This finding provides a quantitative basis for limiting the design pressure of CAS systems.

Practical applicability of the performance map of exergy density isolines

The performance map of exergy density isolines (Figure 7) translates the fundamental thermodynamic relationships into a planning instrument that can be applied directly in the early design phase of CAS systems. For a given target exergy density, the diagram displays the full range of feasible combinations of maximum storage pressure and pressure bandwidth. This enables a trade-off analysis that accounts not only for thermodynamic performance but also for the operating limits of selected compressors and expanders as well as the technical and economic constraints of the CAS. For example, if a specific maximum storage pressure cannot be exceeded due to regulatory or material limitations, the required pressure bandwidth to reach a target exergy density can be read directly from the diagram – and vice versa.

Limitations

The analytical framework developed in this study is intentionally kept general and layout-independent to provide a fundamental understanding of exergy density dependence and to serve as a fast design tool. When applying the results to specific CAES configurations, several limitations must be considered.

Isothermal assumption: The analysis assumes ideal isothermal storage conditions, which yields the theoretical maximum volumetric efficiency and exergy density. In real CAES systems, storage temperatures are typically above ambient and commonly range around 40–50 °C depending on the thermal management of the compression process. Furthermore, transient temperature variations during charging and discharging reduce the usable density change and thus the exergy density, as demonstrated by [15, 25–30]. The extent of this reduction depends on the mass flow rate, geometry, thermal mass and conductivity of the storage vessel, and the ambient conditions.

Layout and system integration: The exergy density discussed here refers exclusively to the thermodynamic potential of the storage vessel itself. In a complete CAES system, the usable exergy also depends on the power unit design (compressor and expander types, number of stages), heat management strategy (TES integration, intercooling), pressure regulation (e.g. throttle valves), and part-load behaviour. These aspects are intentionally excluded to maintain generality but must be considered in detailed system design.

No structural or economic optimization. The optimal maximum storage pressure identified in this study is a purely thermodynamic optimum. In practice, higher pressures entail thicker vessel walls and more stringent safety requirements, leading to increased specific costs (€/m³ storage volume). A techno-economic optimization that balances exergy density against storage vessel cost is therefore required for final design decisions.

5. Conclusion

This study presents a generalized, analytical method for determining the theoretically optimal pressure design for isochoric compressed air storage systems based on real-gas property data for dry air. To this end, the exergy density as a function of maximum storage pressure, pressure bandwidth, and storage temperature, considering both ideal and real gas behaviour. The main conclusions are:

1. The operable pressure bandwidth is the dominant parameter for maximizing volumetric exergy density in isochoric CAS and should be the primary consideration in storage design.
2. For any given combination of pressure bandwidth and storage temperature, a thermodynamically optimal maximum storage pressure exists. This effect is linked to real gas behaviour and cannot be captured by

the ideal gas assumption, which overestimates the exergy density above approximately 120 bar and fails to predict the existence of this optimum. Real gas property data should therefore be used for the design of high-pressure CAS.

3. Higher storage temperatures reduce exergy density and shift the optimal maximum pressure to higher values. Since real storage temperatures typically exceed ambient conditions and fluctuate during operation, thermal effects must be accounted for to avoid undersizing the storage vessel.
4. The performance map of exergy density isolines (Figure 7) provides a practical planning tool for the initial thermodynamic design of isochoric CAS, enabling rapid identification of favourable operating windows independently of specific CAES layouts.

Future work should extend this framework by including transient thermal effects during charging and discharging, coupling the thermodynamic optimum with structural and economic constraints of pressure, and integrating the results into a comprehensive CAES system design and optimization methodology. Moreover, since the developed methodology is based on general thermodynamic principles and real gas property data, it can be transferred to other technically relevant gases such as carbon dioxide, thereby enabling applications in the context of carbon capture and storage.

Nomenclature

e	specific exergy, kJ/kg
e_d	exergy density, kWh/m³
E	exergy, kWh
t	temperature, °C
T	temperature, K
p	pressure, bar
R	universal gas constant, J/(mol K)
n	amount of substance, mol
h	specific enthalpy, kJ/kg
s	specific entropy, kJ/(kg K)
V	volume, m³
Z	compressibility factor, -

Greek symbols

Δ	difference, -
ρ	density, kg/m³

Subscripts and superscripts

a	ambient
max	maximum
min	minimum

Abbreviation

A-CAES	Adiabatic compressed air energy storage
CAES	Compressed air energy storage
CAS	Compressed air storage
D-CAES	Diabatic compressed air energy storage
I-CAES	Isothermal compressed air energy storage
LAES	Liquid air energy storage
TES	Thermal energy storage

References

[1] Quast P. The Huntorf Plant: Over 3 Years operating experience with compressed air caverns. In: U.S. Department of Energy, editor. The Huntorf Plant: Over 3 Years operating experience with compressed air caverns; 1981.

[2] Goodson J. History of first U.S. Compressed Air Energy Storage (CAES) Plant (110-MW-26h): Volume 1: Early CAES Development; Final Report: EPRI; 1992 TR-101751.

[3] Hydrostor Activates World's First Utility-Scale Underwater Compressed Air Energy Storage System; Press Release; 2015.
[4] Mei S, Wang J, Tian F*, et al.* Design and engineering implementation of non-supplementary fired compressed air energy storage system: TICC-500. Sci. China Technol. Sci. 2015; 58(4): 600–11 [https://doi.org/10.1007/s11431-015-5789-0]
[5] Wang J, Lu K, Ma L*, et al.* Overview of Compressed Air Energy Storage and Technology Development. Energies 2017; 10(7): 991 [https://doi.org/10.3390/en10070991]
[6] Geissbühler L, Becattini V, Zanganeh G*, et al.* Pilot-scale demonstration of advanced adiabatic compressed air energy storage, Part 1: Plant description and tests with sensible thermal-energy storage. Journal of Energy Storage 2018; 17: 129–39 [https://doi.org/10.1016/j.est.2018.02.004]
[7] Zhang X, Gao Z, Zhou B*, et al.* Advanced Compressed Air Energy Storage Systems: Fundamentals and Applications. Engineering 2024; 34: 246–69 [https://doi.org/10.1016/j.eng.2023.12.008]
[8] Hydrostor. Projects; 2021.
[9] Tong Z, Cheng Z, Tong S. A review on the development of compressed air energy storage in China: Technical and economic challenges to commercialization. Renewable and Sustainable Energy Reviews 2021; 135: 110178 [https://doi.org/10.1016/j.rser.2020.110178]
[10] U.S. Department of Energy. Technology Strategy Assessment - Compressed Air Energy Storage.
[11] Budt M. Thermodynamische Analyse adiabater Druckluftenergiespeicher unter Berücksichtigung feuchter Luft und Wassereinspritzung mittels dynamischer Simulation. Oberhausen: Karl Maria Laufen 2016.
[12] Yu Q, Wang Q, Tan X, Fang G, Meng J. A review of compressed-air energy storage. Journal of Renewable and Sustainable Energy 2019; 11(4): 42702 [https://doi.org/10.1063/1.5095969]
[13] Jankowski M, Pałac A, Sornek K*, et al.* Status and Development Perspectives of the Compressed Air Energy Storage (CAES) Technologies—A Literature Review. Energies 2024; 17(9): 2064 [https://doi.org/10.3390/en17092064]
[14] Buffa F, Kemble S, Manfrida G, Milazzo A. Exergy and Exergoeconomic Model of a Ground-Based CAES Plant for Peak-Load Energy Production. Energies 2013; 6(2): 1050–67 [https://doi.org/10.3390/en6021050]
[15] He W, Luo X, Evans D*, et al.* Exergy storage of compressed air in cavern and cavern volume estimation of the large-scale compressed air energy storage system. Applied Energy 2017; 208: 745–57 [https://doi.org/10.1016/j.apenergy.2017.09.074]
[16] Sterner M, Stadler I. Energiespeicher - Bedarf, Technologien, Integration. Berlin, Heidelberg: Springer Berlin Heidelberg 2017.
[17] Budt M, Hadam M, Schischke E. Low-temperature Adiabatic Compressed Air Energy Storage for Island Applications. In: Low-temperature Adiabatic Compressed Air Energy Storage for Island Applications; 2019. IEEE; 1–8.
[18] Cárdenas B, Hoskin A, Rouse J, Garvey SD. Wire-wound pressure for small scale CAES. Journal of Energy Storage 2019; 26: 100909 [https://doi.org/10.1016/j.est.2019.100909]
[19] Barbour E, M. Oliveira M, Cardenas B, Pottie D. Exergy analysis of isochoric and isobaric adiabatic compressed air energy storage. IET Renewable Power Gen 2025; 19(1) [https://doi.org/10.1049/rpg2.13184]
[20] Forrest, Katie E. (CONTR). TECHNICAL REPORT TEMPLATE AND USER GUIDE.
[21] White AJ. Theoretical analysis of cavern-related exergy losses for compressed air energy storage systems. Journal of Energy Storage 2024; 81: 110419 [https://doi.org/10.1016/j.est.2024.110419]
[22] Guo C, Xu Y, Zhang X*, et al.* Performance analysis of compressed air energy storage systems considering dynamic characteristics of compressed air storage. Energy 2017; 135: 876–88 [https://doi.org/10.1016/j.energy.2017.06.145]
[23] LibHuAir: Program Libraries for the Calculation of Thermodynamic and Transport Properties for Working Fluids in Energy Conversion Processes. Amberg: KCE-ThermoFluidProperties; 2026. Available from: URL: www.thermofluidprop.com.
[24] Dincer I, Rosen MA. Exergy: Energy, environment and sustainable development. 2nd ed. Oxford: Elsevier Science 2013.
[25] Kim H, Park D, Park E-S, Kim H-M. Numerical modeling and optimization of an insulation system for underground thermal energy storage. Applied Thermal Engineering 2015; 91: 687–93 [https://doi.org/10.1016/j.applthermaleng.2015.08.070]

[26] Sciacovelli A, Li Y, Chen H*, et al.* Dynamic simulation of Adiabatic Compressed Air Energy Storage (A-CAES) plant with integrated thermal storage – Link between components performance and plant performance. Applied Energy 2017; 185: 16–28 [https://doi.org/10.1016/j.apenergy.2016.10.058]
[27] Dooner M, Wang J. Potential Exergy Storage Capacity of Salt Caverns in the Cheshire Basin Using Adiabatic Compressed Air Energy Storage. Entropy 2019; 21(11): 1065 [https://doi.org/10.3390/e21111065]
[28] Guo C, Xu Y, Guo H*, et al.* Comprehensive exergy analysis of the dynamic process of compressed air energy storage system with low-temperature thermal energy storage. Applied Thermal Engineering 2019; 147: 684–93 [https://doi.org/10.1016/j.applthermaleng.2018.10.115]
[29] Zhan J, Ansari OA, Liu W, Chung CY. An accurate bilinear cavern model for compressed air energy storage. Applied Energy 2019; 242: 752–68 [https://doi.org/10.1016/j.apenergy.2019.03.104]
[30] Hadam M. Thermodynamische Analyse eines modularen A-CAES mit umkehrbar betreibbaren Turbo- und Kolbenmaschinen. Ruhr-Universität Bochum 2022.